Fermilab Library
0 1160 0038530 6

217

MIDWESTERN UNIVERSITIES RESEARCH ASSOCIATION

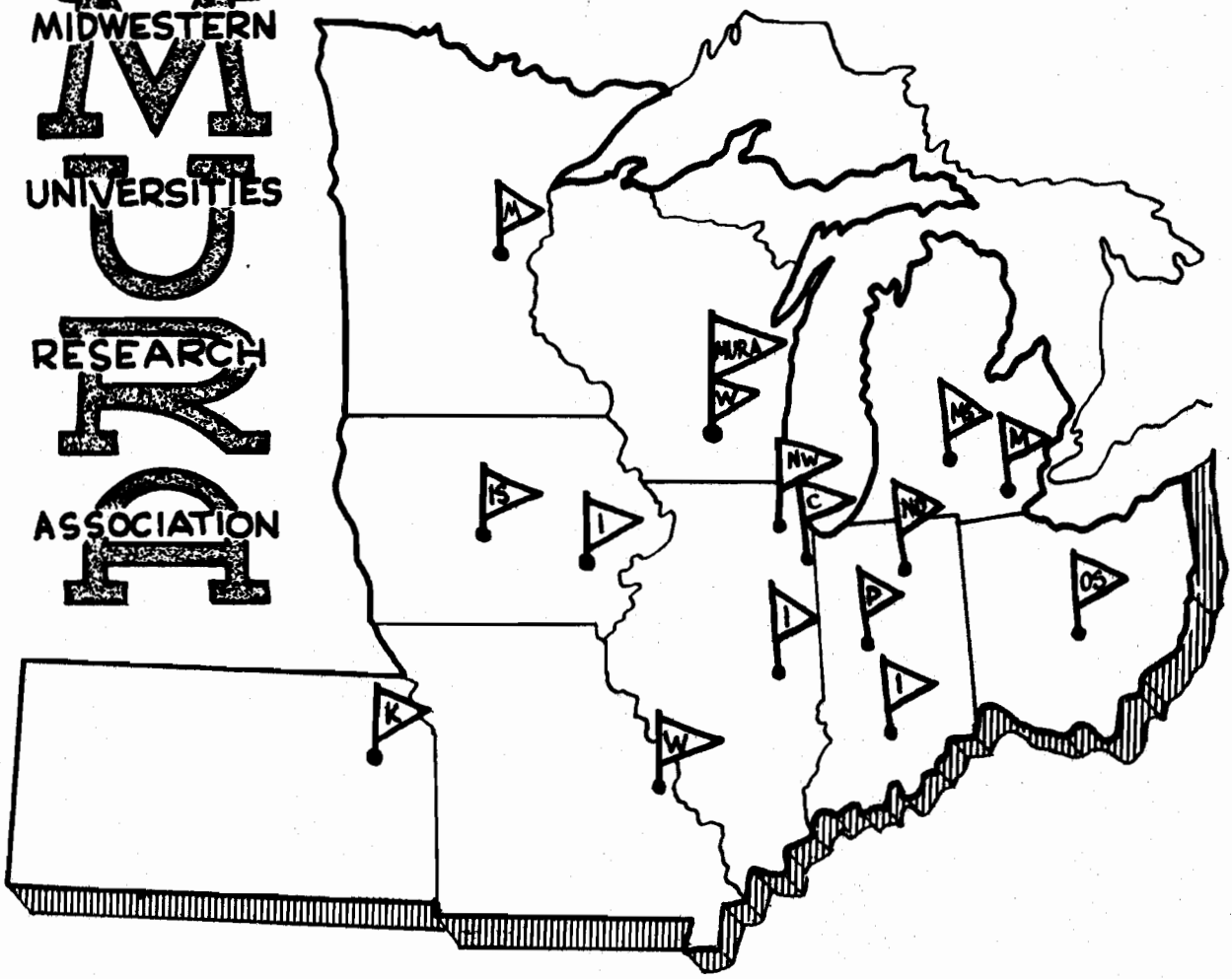

COUPLED NON-LINEAR RESONANCES IN ALTERNATING GRADIENT ACCELERATORS

REPORT **NUMBER** 217

MURA-217

MIDWESTERN UNIVERSITIES RESEARCH ASSOCIATION*
2203 University Avenue - Madison, Wisconsin

COUPLED NON-LINEAR RESONANCES IN ALTERNATING GRADIENT ACCELERATORS

George Parzen**

February 20, 1957

ABSTRACT: The method presented in a previous paper for treating the non-linear resonances in alternating gradient type of high energy accelerators has been extended to treat the two dimensional coupled resonances. The sum resonance $2\nu_y + \nu_x = N$ is treated in detail and the same methods can be applied to the higher order sum resonances. The difference resonances are not treated. The results of the theory are compared with those of a numerical calculation.

* Supported by Contract AEC AT(11-1)-384

** On leave from the University of Notre Dame

I. Introduction

In a previous paper[1] we have treated the non-linear resonances that occur in the radial oscillations of a particle in an alternating gradient accelerator. The vertical motion was not considered. In this paper, the methods presented in the first paper have been extended to treat the two dimensional coupled resonances involving both radial and vertical oscillations.

This paper treats the quadratic sum resonance $2\nu_y + \nu_x = N$ in detail. Higher order sum resonances can be handled in a similar manner. The difference resonances, like the $2\nu_y - \nu_x = 0$ resonance, have an entirely different character and will be treated in a later paper.

As in the case of one-dimensional resonances there are some points in the theory that remain to be cleared up. However, the agreement of the theory with numerical calculations seems to indicate the general correctness of the results.

II. General Description of the Method

The procedure for treating the two dimensional coupled resonances is very similar to that presented in the previous paper[1] (hereafter referred to as Paper I) for the one dimensional radial resonances. The equations of motion are expanded about the equilibrium orbit. If we keep terms up to terms of second order, the expanded equations of motion have the form[2]

$$\left\{ \frac{d^2}{d\theta^2} + E_0 - g_1(\theta) \right\} u = B(\theta)\, u^2 + C(\theta)\, y^2, \tag{2.1a}$$

$$\left\{ \frac{d^2}{d\theta^2} + E_0' - g_2(\theta) \right\} y = D(\theta)\, u\, y. \tag{2.1b}$$

u is the radial displacement of the particle from its equilibrium orbit and y is the vertical displacement. $g_1(\theta)$, $g_2(\theta)$, $B(\theta)$, $C(\theta)$ and $D(\theta)$ are all periodic in θ with the period $2\pi/N$ where

N is the number of sectors in the machine. $D(\theta) = 2\,C(\theta)$ since the equations are Hamiltonian, and $g_1(\theta)$ and $g_2(\theta)$ are defined by requiring that their average value over a period be zero.

As in the one dimensional case, we will investigate the stability properties of Eqs. (2.1) by replacing them by an eigenvalue problem. We will consider the slightly more general equations

$$\left\{\frac{d^2}{d\theta^2} + W - g_1(\theta)\right\} u = B(\theta)\, u^2 + C(\theta)\, y^2, \tag{2.2a}$$

$$\left\{\frac{d^2}{d\theta^2} + W' - g_2(\theta)\right\} y = D(\theta)\, u\, y, \tag{2.2b}$$

and we will ask for what real values of W and W' do Eqs. (2.2) have stable solutions

To solve this eigenvalue problem, we will consider the quadratic terms as perturbations. To carry out this perturbation procedure we must first know the solutions of the unperturbed eigenvalue problem which are the solutions of the following linear equations,

$$\left\{\frac{d^2}{d\theta^2} + E - g_1(\theta)\right\} u = 0, \tag{2.3a}$$

$$\left\{\frac{d^2}{d\theta^2} + E' - g_2(\theta)\right\} y = 0. \tag{2.3b}$$

One can easily solve the eigenvalue problem, that is determine the values of E and E' for which Eqs. (2.3) have stable solutions, since the properties of these linear equations are known (see Paper I).

Equation (2.3a) has stable solutions only for certain values of E and for these "allowed" values of E, the solutions have the form

$$u_\nu(\theta) = e^{i\nu\theta}\, h_\nu(\theta), \tag{2.4}$$

corresponding to the E-value $E_\nu = E(\nu)$. $h_\nu(\theta)$ is periodic in θ with period $2\pi/N$. The allowed E-values are continuous functions of ν but

there are gaps in them which occur at ν = 1/2 N, N, 3/2N, 2N, etc.

Similarly, the stable solutions of Eq. (2.3b) have the form

$$\mathcal{J}_K(\theta) = e^{iK\theta} f_K(\theta) \tag{2.5}$$

corresponding to the allowed E'-value $E'_K = E'(K)$.

Each solution of Eqs. (2.3) corresponds to a set of values of E and E', and we will say that each solution corresponds to an E-point which has the coordinates (E, E'). The allowed E-points of Eqs. (2.3) are indicated in Fig. 1.

The gaps in the allowed E-points are indicated by the shaded regions.

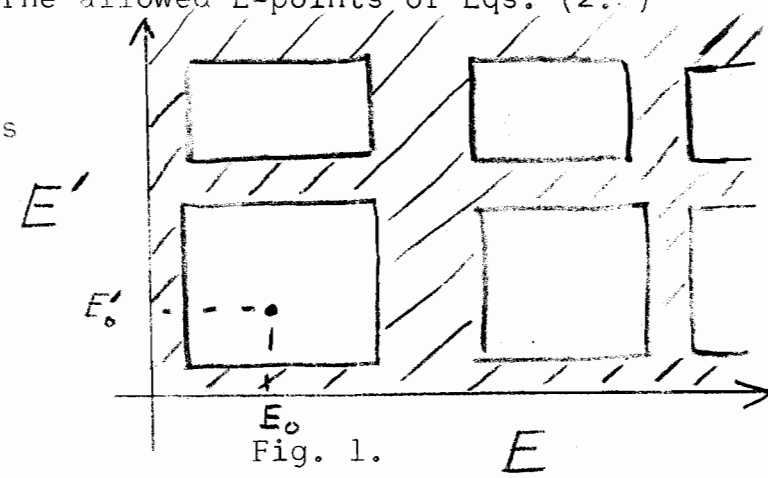

Fig. 1.

For the motion to be stable in the linear theory, the operating E-point (E_o, E_o') must not fall in the gaps. One should also keep in mind that each E-point (E, E' has a μ-tune and y-tune associated with it given by (ν, K) according to Eqs. (2.4) and (2.5). One might note that each E-point is fourfold degenerate.

Now that the unperturbed eigenvalue problem of Eqs. (2.3) has been solved, we will try to solve the eigenvalue problem of the non-linear Eqs. (2.2) by using a perturbation procedure. We will show that the perturbation will cause two new gaps to appear in the allowed E-points as is shown in Fig. 2. These gaps occur around those E-points whose tune lies on the lines $\nu + 2K$ = N and $\nu - 2K$ = 0.

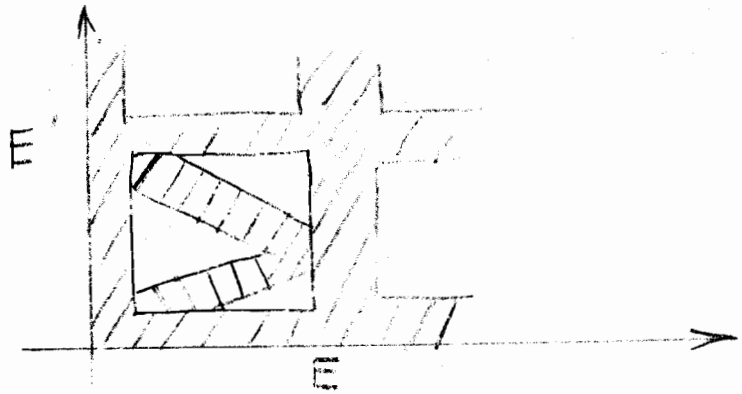

Fig. 2.

We will see that the width of these gaps depends on the amplitude of the motion and will be larger for larger amplitudes.

The question of stability is answered by where the point (E_o, E_o') falls in Fig. 2., since our particle motion is given by solving Eqs. (2.2) for $W = E_o$ and $W' = E_o'$. If (E_o, E_o') does not fall in the gaps, the motion is stable. However, if the amplitude of the motion is increased, the gaps become larger and (E_o, E_o') will eventually lie inside a gap and the motion becomes unstable. This will determine the stability limit amplitudes.

To solve Eqs. (2.2) for u and y we will expand u and y in terms of the solutions $u_\nu(\theta)$ and $y_K(\theta)$ of the linear equations (2.3). As in Paper I, we form a discrete orthonormal set out of the functions u_ν and y_K by imposing the boundary condition that they be periodic between $\theta = 0$ and $\theta = T$ where T is some arbitrarily large angle which we will eventually let become infinite.

The solutions of the linear Eqs. (2.3) can then be written as

$$u_\nu = \frac{e^{i\nu\theta}}{\sqrt{T}} h_\nu(\theta), \tag{2.6a}$$

$$y_K = \frac{e^{iK\theta}}{\sqrt{T}} f_K(\theta), \tag{2.6b}$$

and they form two orthonormal sets,

$$\int_0^T d\theta\, u_{\nu'}^*(\theta)\, u_\nu(\theta) = \delta_{\nu'\nu}, \tag{2.7a}$$

$$\int_0^T d\theta\, y^*_{K'}(\theta)\, y_K(\theta) = \delta_{KK'} , \tag{2.7b}$$

if $h_\nu(\theta)$ and $f_K(\theta)$ are so normalized that

$$\frac{N}{2\pi}\int_0^{\frac{2\pi}{N}} d\theta\, |h_\nu|^2 = 1 , \tag{2.8a}$$

and

$$\frac{N}{2\pi}\int_0^{2\pi/N} d\theta\, |f_K|^2 = 1 \tag{2.8b}$$

Now expand u in u_ν and y in y_K

$$u = \sum_{\nu_i} a_{\nu_i}\, u_{\nu_i}(\theta), \tag{2.9a}$$

$$y = \sum_{K_i} b_{K_i}\, y_{K_i}(\theta) \tag{2.9b}$$

and by putting this expansion in Eqs. (2.3), we get the equations for a_ν and b_K ,

$$(W - E_{\nu_i})\, a_{\nu_i} = \sum_{j\ell} B_{\nu_i,\nu_j\nu_\ell}\, a_{\nu_j}\, a_{\nu_\ell} + \sum_{j\ell} C_{\nu_i,K_j K_\ell}\, b_{K_j}\, b_{K_\ell} , \tag{2.10a}$$

and

$$(W' - E'_{K_i})\, b_{K_i} = \sum_{j\ell} D_{K_i,\nu_j K_\ell}\, a_{\nu_j}\, b_{K_\ell} , \tag{2.10b}$$

where

$$B_{\nu_i\nu_j\nu_\ell} = \int_0^T d\theta\, u^*_{\nu_i}\, B(\theta)\, u_{\nu_j}\, u_{\nu_\ell} , \tag{2.11}$$

$$C_{\nu_i,K_j K_\ell} = \int_0^T d\theta\, u^*_{\nu_i}\, C(\theta)\, y_{K_j}\, y_{K_\ell} , \tag{2.12}$$

and

$$D_{K_i\nu_j K_\ell} = \int_0^T d\theta\, y^*_{K_i}\, D(\theta)\, u_{\nu_j}\, y_{K_\ell} . \tag{2.13}$$

Now we will solve Eqs. (2.10) for a_ν and b_K by a perturbation procedure. Consider the E-point (E_s, E' of the linear equations (2.3) which has the tune (ν_s, K_s), and which corresponds to the

solution $\mathcal{U} = a\mathcal{U}_{\nu_s} + a^*\mathcal{U}_{-\nu_s}$, $y = b\,\mathcal{Y}_{K_s} + b^*\mathcal{Y}_{-K_s}$. This E-point will be shifted by our non-linear perturbation. To find this shift, we will solve Eqs. (2.10), by assuming that in the expansions (2.9) for $\mathcal{U}$ and y, only a_{ν_s}, $a_{-\nu_s}$, b_{K_s} and b_{-K_s} are large and all the other a_ν and b_K are small.

Thus to first approximation Eqs. (2.10) become

$$(W-E_i)a_i = \sum_{s's''}\left(B_{i,s's''}a_{s'}a_{s''} + C_{i,s's''}b_{s'}b_{s''}\right), \tag{2.14a}$$

$$(W'-E_i')b_i = \sum_{s's''} D_{i,s's''}a_{s'}b_{s''} \tag{2.14b}$$

In Eqs. (2.14) and in later work, we shall use the notation $E_{\nu_s} = E_s$, $\mathcal{U}_{\nu_s} = \mathcal{U}_s$, $B_{\nu_i,\nu_j\nu_k} = B_{i,jk}$ and $-\nu_s = \nu_{\bar{s}}$. In the sums of Eqs. (2.14), s' and s'' can take on only two values, s and $\bar{s} = -s$

The matrix element $B_{i,j\ell}$ will vanish (see Paper I) unless

$$\nu_i = \nu_j + \nu_\ell + \omega_n, \tag{2.15}$$

where $\omega_n = nN$, $n = 0, \pm 1, \pm 2 \ldots$

Similarly $C_{i,j\ell}$ will vanish unless

$$\nu_i = K_i + K_\ell + \omega_n, \tag{2.16}$$

and $D_{i,j\ell}$ will vanish unless

$$K_i = \nu_j + K_\ell + \omega_n. \tag{2.17}$$

The shift in the E-point (E_s, E_s' having the tune (ν_s, K_s) is given by Eqs. (2.14) by putting i = s. For i = s, Eqs. (2.14) become

$$(W-E_s)a_s = \sum_{s's''}\left\{B_{s,s's''}a_{s'}a_{s''} + C_{s,s's''}b_{s'}b_{s''}\right\}, \tag{2.18a}$$

$$(W'-E_s')b_s = \sum_{s's''} D_{s,s's''}a_{s'}b_{s''} \tag{2.18b}$$

Now using the conditions (2.15) to (2.17), we will see that matrix elements will vanish unless the tunes (ν_s, K_s) lies on certain lines in a (ν, K) diagram, which we will soon indicate. If the tune does not lie in these lines, the matrix elements vanish and by Eqs. (2.18) the E-point (E_s, E_s') corresponding to this tune is not shifted as $(W - E_s) = W' - E_s' = 0$. If the tune ($\nu_s$, K_s) does lie in these lines for which the matrix elements do not vanish, then by Eqs. (2.18), the E-point (E_s, E_s') corresponding to this tune is shifted and we will see later that the E-point is split into two points. We will see that these lines on which the E-points get split are the resonance lines at which the motion becomes unstable.

Using the conditions (2.15) to (2.17) one can see that $B_{s,s's''}$ will vanish unless

$$\nu_s = \frac{1}{3}\omega_n \tag{2.19}$$

$C_{s,s's''}$ will vanish unless

$$\nu_s \pm 2K_s = \omega_n \tag{2.20}$$

$D_{s,s's''}$ will vanish unless

$$\nu_s \pm 2K_s = \omega_n \tag{2.21}$$

The matrix elements also do not vanish if $\nu_s = \omega_n$; but as this tune is already unstable in the linear case, we will not consider it. We will see that Eq. (2.19) shows that $B(\theta)\mu^2$ term in Eqs. (2.1) causes $\nu_s = (1/3)\omega_n$ resonance, while the $C(\theta)\, y^2$ and $D(\theta)\, \mu y$ terms cause the coupled resonances $\nu_s \pm 2K_s = \omega_n$. The absence of a y^2 term in Eq. (2.16) shows that there is no $K_s = (1/3)\omega_n$ resonance which has been checked in computer calculations[3] done by L. J. Laslett.

In this paper we will restrict our attention to the $\nu_s + 2K_s = \omega_n$ sum resonance. Sum resonances due to higher order terms in the

Eqs. (2.1) can be handled in the same way. Difference resonances are considerably different in character and will be treated in a later paper.

Let us consider then the E-points (E_s, E_s') whose tune (ν_s, K_s) lies on the line $\nu_s + 2K_s = N$. We will treat the case $\omega_h = \omega_1 = N$, but the general ω_h case is quite similar. The shift in these E-points is given by Eqs. (2.18) which now become

$$(W - E_s)\, a_s = C_{s,\bar{s}\bar{s}}\, b_{\bar{s}}^2, \tag{2.22a}$$

$$(W' - E_s')\, b_s = D_{s,\bar{s}\bar{s}}\, a_{\bar{s}}\, b_{\bar{s}}. \tag{2.22b}$$

Most of the matrix elements in Eqs. (2.18) vanish because $\nu_s + 2K_s = N$ and because of conditions (2.19) to (2.21). One should notice that $D_{s,\bar{s}\bar{s}} = 2\, C_{s,\bar{s}\bar{s}}$ by Eqs. (2.12) and (2.13) and since $D(\theta) = 2\,(\theta)$

$(W - E_s)$ and $(W' - E_s')$ which give the shift in the E-point (E_s, E_s') can be solved for from Eqs. (2.22). The magnitudes of ($W - E_s$) and ($W' - E_s'$) are given by

$$|W - E_s| = |C_{s,\bar{s}\bar{s}}|\; |b_s^2 / a_s|, \tag{2.23a}$$

$$|W' - E_s'| = 2\,|C_{s,\bar{s}\bar{s}}|\; |a_s|. \tag{2.23b}$$

The magnitude of the shift depends on the amplitudes of the motion, b_s and a_s.

We will now show that because of Eqs. (2.22), ($W - E_s$) and ($W' - E_s'$) must have the same sign.

From Eqs. (2.22) we see that

$$\mathrm{ph}\,(W - E_s) = \mathrm{ph}\, C_{s,\bar{s}\bar{s}} - 2\beta - \alpha, \tag{2.24a}$$

and

$$ph(W'-E_s) = ph\, C_{s,5\bar{5}} - 2\beta - \alpha \qquad (2.24b)$$

where ph means the phase of a_s, and ph $a_s = \alpha$, and ph $b_s = \beta$.

Thus ph $(W-E_s)$ = ph $(W'-E_s')$ and $(W-E_s)$, $(W'-E_s')$ have the same sign. This has the consequence that the E-point (E_s, E_s') for given amplitude a_s and b_s is split into just two points as is shown in Fig. 3.

Each E-point in the line is split into two points. A gap appears in the E-point diagram around the line $\nu_s + 2K_s = N$. The size of the gap depends on the amplitudes of the motion a_s and b_s and is given by Eqs. (2.33)

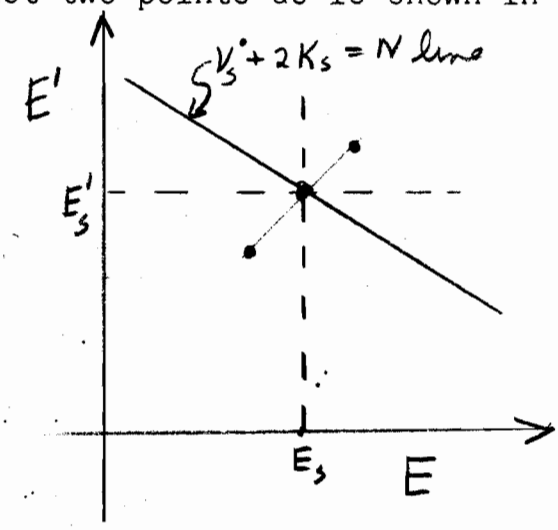

Fig. 3.

Eqs. (2.18) seem to show that an E-point whose tune lies very near the resonance line $\nu_s + 2K_s = N$ is not shifted. This is not so. The situation is similar to that in the one dimensional case and Eqs. (2.18) are not valid for E-points very near the resonance line but not exactly on the resonance line. Some discussion of this point is given in Paper I. We shall assume here without any further proof that these E-points will be shifted to someplace outside the gap computed by considering the shift of the E-points on the resonance line.

We can now discuss the question of stability. If the operating point (E_o, E_o') lies outside the gap that appears around the line $\nu_s + 2K_s = N$, then the motion is stable. By increasing a_s and b_s we can increase the size of the gap until (E_o, E_o') lies inside

the gap and the motion becomes unstable. The limiting case is when (E_o, E_o^1) lies on the edge of the gap as is shown in Fig. 4. This will happen when some E-point (E_s, E_s') on the resonance line $\nu_s + 2K_s = N$ is shifted to the operating point (E_o, E_o').

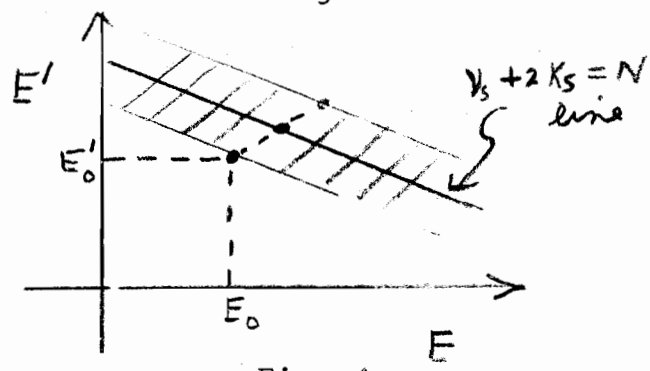

Fig. 4.

Which E-point (E_s, E_s') reaches the operating point (E_o, E_o') depends on the relative size of a_s and b_s according to Eqs. (2.33). If the amplitudes a_s and b_s are such as to cause some particular E-point (E_s, E_s') on the resonance line to reach the operating point (E_o, E_o'), then the effective tune of the motion will have changed from (ν_o, K_o) to (ν_s, K_s).

There is then not just one set of stability limit amplitudes a_s, b_s but many sets depending on which tune on the resonance line (ν_s, K_s) the motion is driven to; which, in turn, depends on the relative size and phase of a_s and b_s.

The stability limit amplitudes a_s, b_s to drive the tune of the motion to (ν_s, K_s) which lies on the resonance line $\nu_s + 2K_s = N$ can be found from Eqs. (2.22) by putting $W = E_o$ and $W' = E_o'$ Thus we get

$$|a_s| = \frac{|E_o' - E_s'|}{2|C_{s,\bar{s}\bar{s}}|}, \tag{2.25a}$$

$$|b_s| = \left\{ \frac{|E_o - E_s|\,|E_o' - E_s'|}{2|C_{s,\bar{s}\bar{s}}|^2} \right\}^{\frac{1}{2}} \tag{2.25b}$$

One should note that it is not possible to drive the operating tune (ν_o, K_o) to all the tunes in the resonance line. Because the

E-points on the resonance line can be shifted only into the first and third quadrants as shown in Fig. 3, one can see that only the tunes shown in Fig. 5 are reachable.

To get some idea of how a_s and b_s depend on the tune (ν_s, K_s) that the motion is driven to, we would like to give some approximate formulas for a_s and b_s.

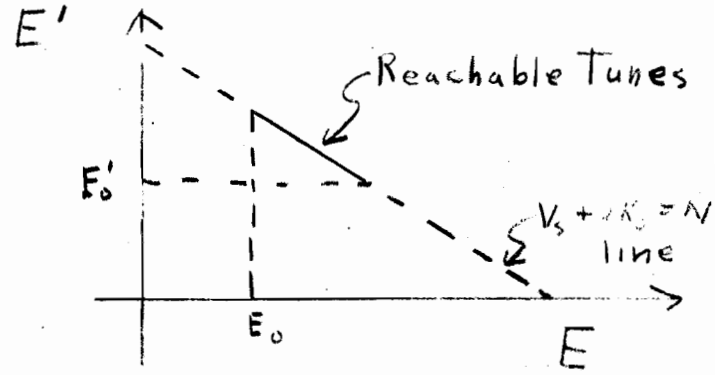

Fig. 5.

In Eqs. (2.25) we shall make the following approximations. We shall put $E_s \simeq \nu_s^2$, $E_s' \simeq K_s^2$ and in computing $C_{s,35}$, we shall put $\mu_\nu(\theta) \simeq e^{i\nu\theta}/\sqrt{T}$, $\eta_K(\theta) \simeq e^{iK\theta}/\sqrt{T}$.
These relations would be exact if $g_1(\theta) = g_2(\theta) = 0$ in Eqs. (2.1) and are roughly true in most cases met in practice. We then get[4] for a_s and b_s,

$$|a_s| = \frac{N^2}{|C_1|} \frac{K_0}{N} \frac{K_s - K_0}{N} , \tag{2.26a}$$

$$|b_s| = \frac{N^2}{|C_1|} \sqrt{\frac{2\nu_0 K_0}{N^2}} \sqrt{\frac{(K_s - K_0)(\nu_s - \nu_0)}{N^2}} \tag{2.26b}$$

where C_1 is the first harmonic in the expansion of $C(\theta)$, $C(\theta) = \sum_n C_n e^{i\omega_n \theta}$, and we have assumed that (ν_0, K_0) is very close to the resonance line so that $\nu_0 + 2K_0 \simeq N$. We have also omitted all factors of $\sqrt{T}$, and shall do so hereafter, as all such factors must cancel in the final answer.

We can use Eqs. (2.26) to plot $|a_s|$, $|b_s|$ against the tune K_s , or we can plot $|b_s|$ against $|a_s|$. This last curve is the more important one and is indicated in Fig. 6.

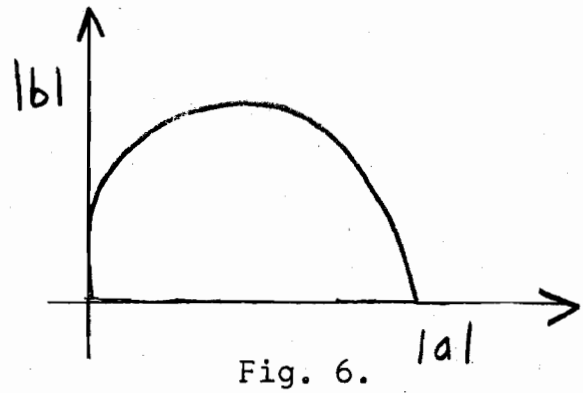

Fig. 6.

The maximum value of $|a|$ is given by

$$a_{max} = \frac{N^2}{|c_1|} \frac{K_0}{N} \cdot \varepsilon , \tag{2.27}$$

where ε measures how far (ν_0, K_0) is from the resonance line and is defined by $\varepsilon = \frac{1}{2} \left| 1 - \nu_0/N - 2K_0/N \right|$

The maximum value of $|a|$ occurs at the tune $(K_s - K_0)/N = \varepsilon$.

The maximum value of $|b|$ occurs at the tune $(K_s - K_0)/N = \frac{1}{2}\varepsilon$ and is given by

$$b_{max} = \sqrt{\nu_0/K_0}\; a_{max} \tag{2.28}$$

The curve shown in Fig. 6 has the equation

$$\frac{b}{b_{max}} = 2 \left\{ \frac{a}{a_{max}} \left(1 - \frac{a}{a_{max}} \right) \right\}^{\frac{1}{2}} \tag{2.29}$$

We should point out here that a portion of the curve in Fig. 6 is not accurate. This is the portion near the origin where $|b/a| \gg 1$. Because $b_s \gg a_s$, higher order terms neglected in the theory become important. Actually $|b|$ does not go to zero when $|a| \to 0$. However, it has been estimated that the breakdown of the theory occurs only near the origin for $a \ll a_{max}$.

III. The Stability Surface

The results of the preceding section for the stability limit amplitudes can be better understood by introducing the idea of the

stability surface which we will develop now. We will start by discussing the stability limit orbits.

According to the results of section II, there is not one but many stability limit orbits. The stability limit orbits have different tunes (ν_s, K_s), though all the tunes lie in the resonance line $\nu_s + 2K_s = N$ and must lie in the region shown in Fig. 5. The stability limit amplitudes, a_s and b_s, depend on the tune of the orbit and are given by Eqs. (2.25). The orbits themselves follow from the expansions, Eqs. (2.9), and are given by

$$u = a_s u_s(\theta) + a_s^* u_s^*(\theta), \tag{3.1a}$$

$$y = b_s y_s(\theta) + b_s^* y_s^*(\theta). \tag{3.1b}$$

$u' = du/d\theta$ and $y' = dy/d\theta$ can then be calculated by differentiating Eqs. (3.1)

Now each stability limit orbit, $u = u(\theta)$, $y = y(\theta)$, $u = u'(\theta)$, $y = y'(\theta)$ can be considered as a curve in four dimensional space. We will show that all the stability limit orbits lie on a closed 4-dimensional surface and they completely fill this surface. This 4-dimensional surface we will call the stability surface.

We will assume that if the motion is started at a point (u, y, u', y') outside this 4-dimensional surface, then it will be unstable. Thus the stability surface will give us the region of phase space that is stable.

We will now obtain the above results. In order to have a concrete example before our eyes, we would like to treat the special case with no AG in the linear terms, which means $g_1(\theta) = g_2(\theta)$ in Eqs. (2.1). Our results however will be quite general. For this

case the linear solutions are simple exponentials $u_\nu = e^{i\nu\theta}$, $y_K = e^{iK\theta}$, and $E_\nu = \nu^2$, $E_K = K^2$.

For this case the stability limit orbits are given by

$$u = A \cos(\nu\theta + \alpha) \tag{3.2a}$$

$$y = B \cos(K\theta + \beta), \tag{3.2b}$$

$$u' = -\nu A \sin(\nu\theta + \alpha) \tag{3.2c}$$

$$y' = -K B \sin(K\theta + \beta), \tag{3.2d}$$

where $A = 2|a|$, $B = 2|b|$, $\alpha = \mathrm{ph}\, a$ and $\beta = \mathrm{ph}\, b$.

Let us note that the parameters that occur in Eqs.(3.2 are not all independent. ν and K are related by $\nu + 2K = N$. A and B determined by the tune (ν, K) according to Eqs. (2.2b). And α and β are related by Eq. (2.24a),

$$\mathrm{ph}\,(E_0 - E_s) = p\,C - 2\beta - \alpha \tag{3.3}$$

For example, if E_0 is below the resonance line, so that $\mathrm{ph}(E_0 - E_s) = \pi$, and if $C(\theta) = 2|C_1| \sin N\theta$, so that $\mathrm{ph}\, C_1 = -\frac{\pi}{2}$, then we would get $\alpha + 2\beta = \pi/2$.

Thus there are only three independent parameters in Eqs. (3.2) which we can take as ν, θ and α. Eqs. (3.2) can then be considered as a set of four equations for u, y, u', y' involving three parameters ν, θ, α and are thus the parametric representation of a surface in the 4-dimensional space of u, y, u', y'. Theoretically, ν, θ, and α could be eliminated from Eqs. (3.2) to give a single relation between u, y, u' and y'. Thus we have shown that the set of stability limit orbits form a surface.

In the next section we will present ways of picturing this 4-dimensional stability surface. We would like to remark here that we have not really shown that the surface we found is the true stability surface in the sense that every point outside the surface is unstable. However, as the surface is made up of the stability limit orbits, it seems plausible that either it is the true stability surface or it is very close to the true stability surface.

IV. Sections of the Stability Surface.

One way of picturing the 4-dimensional stability surface is to pass a "plane" through the surface and examine the curve which is the intersection of this plane with the stability surface. For example we can take the plane defined by $u' = y' = 0$, and we can find the points on the stability surface that lie in this plane. The two dimensional curves we so obtain should give us some idea of what the stability surface looks like.

These sections also have the advantage of being closely connected with stability calculations as done on a computer. In the usual computations done on a computer like the ILLIAC to measure the stability limits, such a section is usually traced out at least partially.

To illustrate these sections we will treat the special case mentioned in Section III where $g_1(\theta) = g_2(\theta) = 0$ in Eqs (2.1) and $C(\theta) = 2|c_1| \sin N\theta$.

Let us now find the section defined by the plane $u' = y' = 0$. The stability surface is given by Eqs. (3.2) with the added restriction that $\alpha + 2\beta = \pi/2$. Let us just find those values of ν, θ, δ which make $u' = y' = 0$ and then we can find those points in the surface that have $u' = y' = 0$.

To make $u' = y' = 0$, the parameters ν, θ, and α must obey the conditions,

$$\nu\theta + \alpha = 0 \quad \text{or} \quad \pi, \tag{4.1a}$$

$$K\theta + \beta = 0 \quad \text{or} \quad \pi. \tag{4.1b}$$

Let us first assume that $\nu\theta + \alpha = 0$, and $K\theta + \beta = 0$. Then multiplying Eq. (4.1b) by two and adding to Eq. (4.14), we find that $(\nu + 2K)\theta + (\alpha + 2\beta) = 0$. Now using the relations $\nu + 2K = N$ and $\alpha + \beta = \pi/2$, we find that $N\theta = -\pi/2$. This means that at the angle $N\theta = -\pi/2$, there are points on the stability surface at which $u' = y' = 0$ and at these points $u = A$ and $y = B$. Note that A and B depend on ν according to Eqs. (2.26). Thus as ν is varied we find the points u, y shown in the first quadrant of Fig. 6.

This curve is just the b against a curve of Fig. 6.

By treating the other possible cases according to Eqs. (4.1) we find the rest of the section $u' = y' = 0$ as shown in Fig. 7. One might note that each point in the curve has definite θ associated with it.

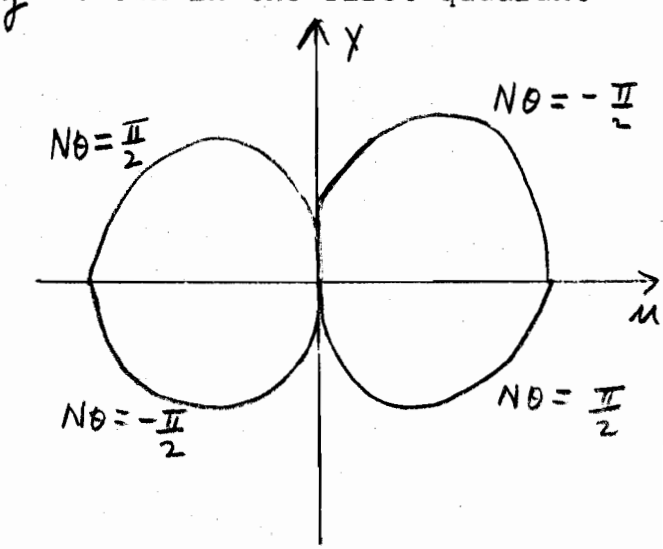

Fig. 7.

The curve in Fig. 7 is instructive for the calculation of stability limits on a computer. If in the computer calculations, one starts with initial conditions of $u' = y' = 0$ at $\theta = 0$, then one will be unable to find points on the stability surface since according to Fig. 7, the points on the stability surface

having $u' = y' = 0$ occur at $N\theta = \pm \frac{\pi}{2}$. Computations on the computer are done by starting with $u' = y' = 0$ at $\theta = 0$ and at some (u, y) which is outside the stable region. One then moves (u, y) in towards the stable region until one finds a stable motion. The point so found will lie somewhere inside the stability surface, since the points in the surface have $N\theta = \pm \pi/2$.

We would like to also present the section corresponding to the plane $u = y' = 0$. This is shown in Fig. 8. The curve is just a plot of B against νA, and can be found from Eqs. (2.26). This section was easier to treat in our computer calculations as there are points in the surface having $u = y' = 0$ at $\theta = 0$.

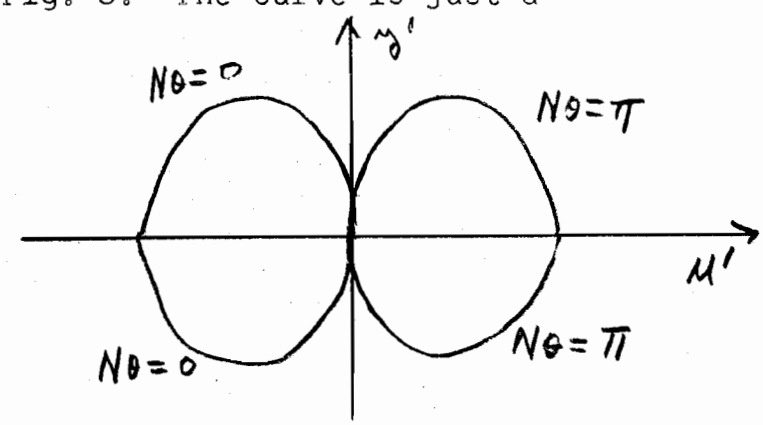

Fig. 8.

V. Comparison with Numerical Calculations

To compare the theory with numerical calculations, we treated the following set of equations,

$$\left\{\frac{d^2}{d\theta^2} + E_0\right\} u = B(\theta)\, u^2 + C(\theta)\, y^2, \tag{5.1a}$$

$$\left\{\frac{d^2}{d\theta^2} + E_0'\right\} y = 2\, C(\theta)\, u\, y, \tag{5.1b}$$

where we put $B(\theta) = 2\,|B_1| \sin N\theta$,

$C(\theta) = 2\,|C_1| \sin N\theta$ and $E_0/N^2 = .05886$,

$E_0'/N^2 = .1232$, and

$|B_1| = |C_1| = .0806$.

These numbers and the form of the equations have been chosen to resemble the actual equations for a spiral sector[5] FFAG type of accelerator. The only change was to omit the AG in the linear

term which was done to simplify the calculations.

For the above numbers $\nu_0/N = .2426$ and $K_0/N = .351$ so that $2K_0 + \nu_0 = .9946\,N$ and we are close to the $2\kappa + \nu = N$ resonance.

Using the ILLIAC computer at the University of Illinois, we have traced out the section of the stability surface corresponding to the plane $\mu = y' = 0$. The results are shown in Fig. 9. Since it is convenient to start the calculations on the computer at $\theta = 0$, we can find points in the section which lie in the second and third quadrants of Fig. 9. The section-points in the first and fourth quadrants correspond to $N\theta = \pi$ and when the computer approaches the stability region starting from the right of it, it can only find points well inside the surface as is shown.

We can also make a comparison between the stability limit orbits as predicted by the theory and as computed on the computer. If we start the motion on some point in the stability surface, then the particle will move in a stability limit orbit which lies entirely in this surface. The equation of this orbit for Eqs. (5.1) are given by Eqs. (3.2). The stability limit orbits are simple sine curves for this case.

In Figs. 10 and 11 we have plotted μ against θ and y against θ for the stability limit orbit which the particle will follow if it is started at the point $\mu = 0$, $y = .185$, $\mu' = -.0652$, $y' = 0$ which is a point in the stability surface. This is the stability limit orbit in which y reaches its largest value. According to Eq. (2.28), the largest stable value if y is .20 for our case which is to be compared with the computed value of .185. This orbit has the tune $(K_s - K_0)/N = \epsilon/2 = .014$ and $(\nu_s - \nu_0)/N = .027$ according to theory, and the computed tune agrees faily well as the curves show.

Fig. 9. A comparison of the theory with numerical calculations for the section of the stability surface corresponding to the plane $\mu = \nu = 0$. The curves are theoretical the points are computed numerically. The points with a dot on them do not lie on the stability surface but indicate the stability boundary at $\theta = 0$.

Fig. 10. The stability limit orbit corresponding to the initial conditions $u = 0$, $y = .185$, $u' = -.0652$, $y' = 0$. The radial displacement u is plotted against θ. The solid curve is the numerically computed result; the broken curve is the theoretical result.

Fig. 11. The stability limit orbit corresponding to the initial conditions $u = 0$, $y = .185$, $u' = -.0652$, $y' = 0$. The vertical displacement y is plotted against θ. The solid curve is the numerically computed result; the broken curve is the theoretical result.

References

1. G. Parzen, MURA Report, MURA-200

2. F. T. Cole, MURA Report, MURA/FTC-3

3. L. J. Laslett, MURA Report MURA/LJL-Int.-11
The absence of this resonance has also been pointed out by Hagedorn, Hine and Schoch, CERN Symposium 1956.

4. The results of Eqs. (2.26) for the special case when $\nu_s = \nu_o$, were previously obtained by Dr. Laslett and Dr. Sessler (unpublished).

5. Symon, Kerst, Jones, Laslett and Terwilliger
Physical Review 103, 1837 (1956)

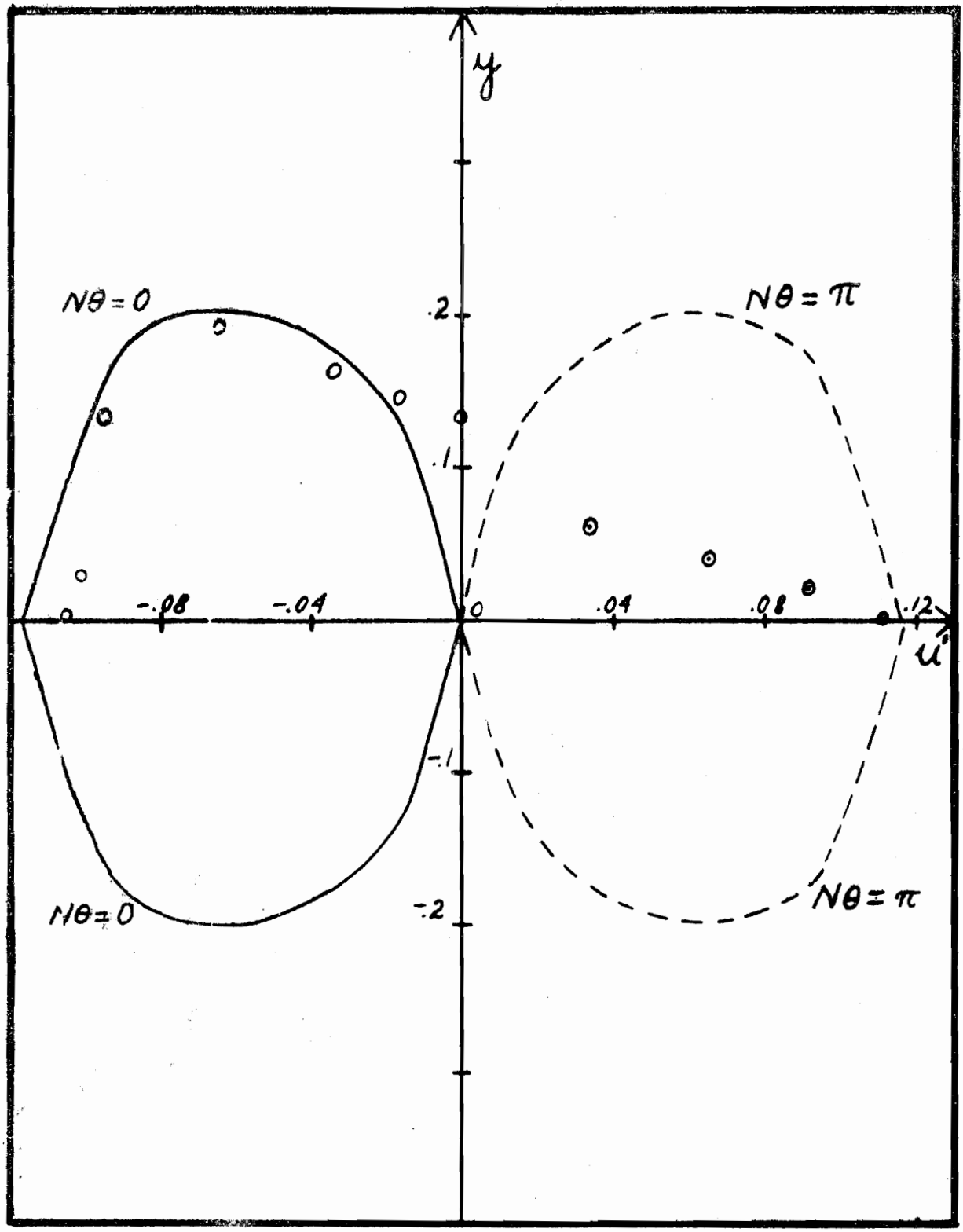

Figure 9

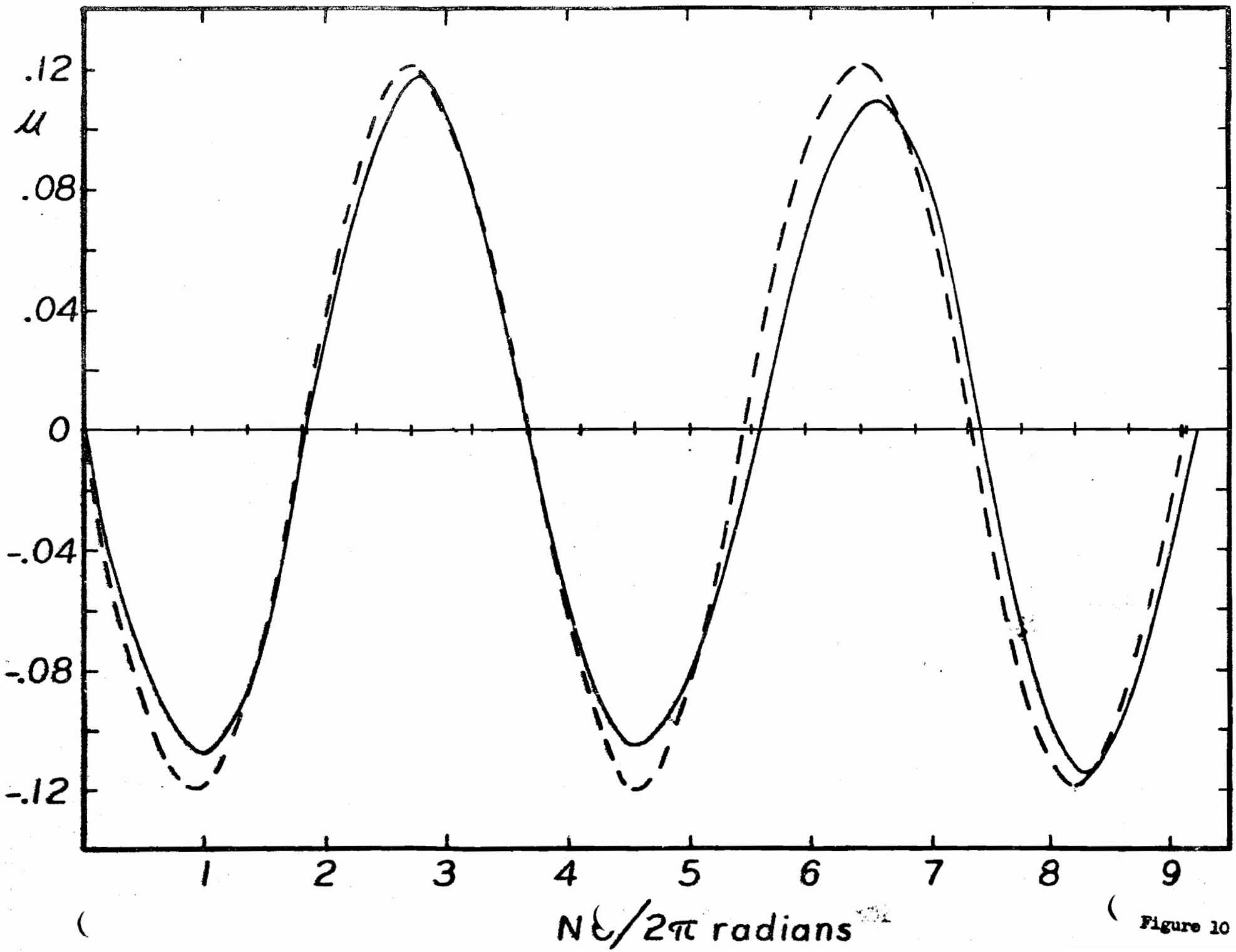

Figure 10

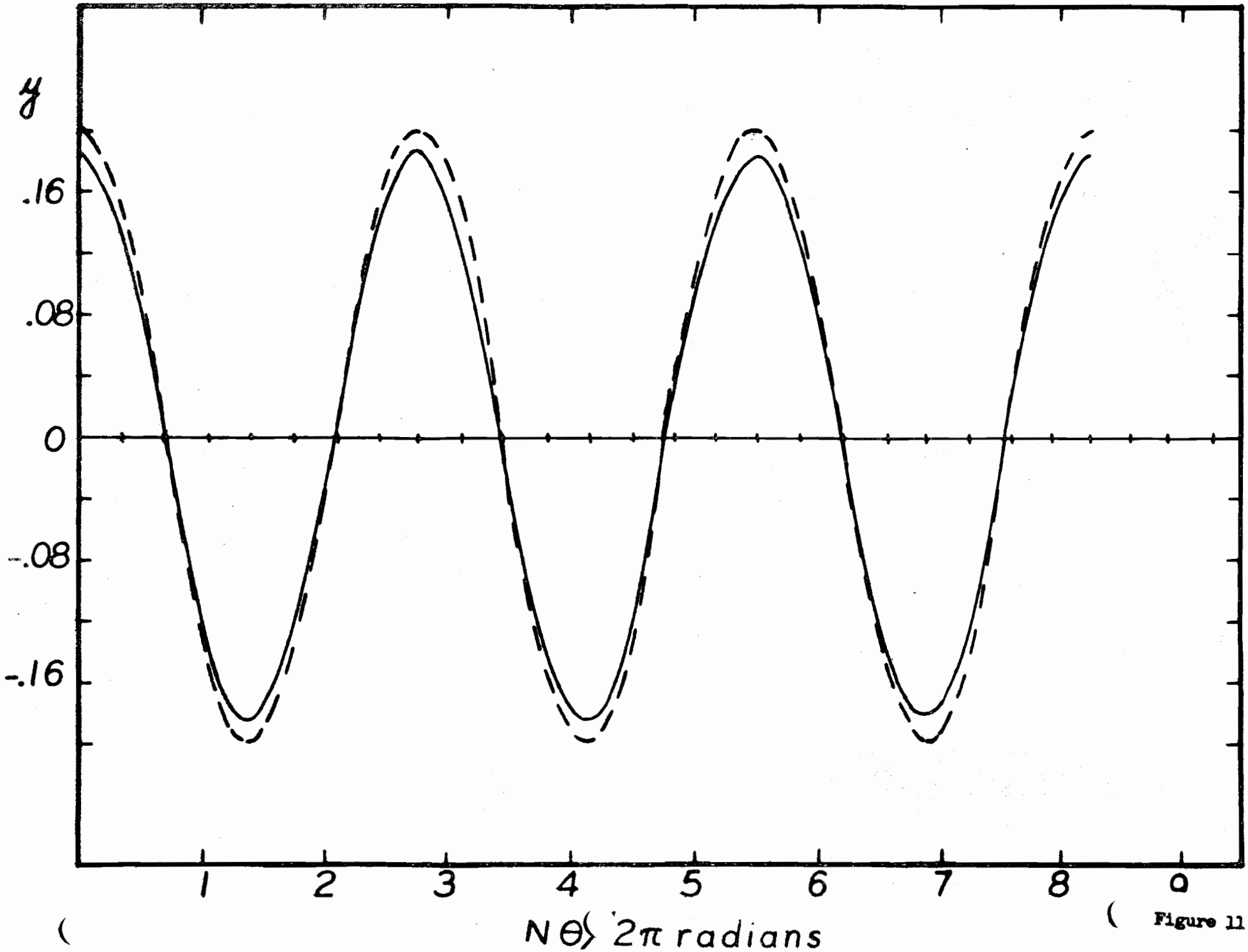

Figure 11